THE JOURNAL OF BIOLOGICAL CHEMISTRY
Vol. 273, No. 47, Issue of November 20, pp. 31145–31152, 1998
Printed in U.S.A.

The Binding of Calcium to the B-repeat Segment of SdrD, a Cell Surface Protein of *Staphylococcus aureus**

(Received for publication, July 28, 1998, and in revised form, August 27, 1998)

Elisabet Josefsson‡, David O'Connell‡, Timothy J. Foster‡, Isabelle Durussel§, and Jos A. Cox§¶

From the ‡Department of Microbiology, Moyne Institute of Preventive Medicine, University of Dublin, Trinity College, Dublin 2, Republic of Ireland and §Department of Biochemistry, University of Geneva, 1211 Geneva 4, Switzerland

In the Sdr family of *Staphylococcus aureus* cell surface proteins, three recently cloned members (Josefsson, E., McCrea, K., Ni Eidhin, D., O'Connell, D., Cox, J. A., Hook, M., and Foster, T. (1998) *Microbiology,* in press) display variable numbers of B-repeats, *i.e.* segments of 110–113 residues that probably make up one folding unit. Each B-repeat contains one conserved EF-hand motif and two acidic stretches. Equilibrium dialysis revealed that segment B1–B5 of SrdD contains 14 Ca^{2+}-binding sites with high affinity ($[Ca^{2+}]_{0.5}$, 4 μM), whereas flow dialysis yielded 5 sites of high affinity (class I) and 10 of low affinity (class II). The discrepancy could be explained by the slow induction of high affinity in the class II sites. Kinetic experiments using fluorescent Ca^{2+} indicators corroborated slow binding of Ca^{2+} at the latter sites. Circular dichroism and Trp fluorescence showed that, whereas the Ca^{2+} form is well folded, the metal-free form seems strongly disorganized. The Ca^{2+}-induced conformational changes comprise both fast and slow steps, giving thus a structural support for the induction of class II Ca^{2+}-binding sites. The B-repeats may act as rulers or springs that modulate the distance between the interactive A region and the bacterial cell surface.

There are two major steps in the pathogenesis of infections caused by *Staphylococcus aureus*: (i) adherence of bacteria to the surface of damaged tissue or implanted medical devices and (ii) synthesis of toxins that damage tissue and cause symptoms of disease (1). *S. aureus* expresses a variety of cell surface-associated proteins (adhesins) that interact with various components of the extracellular matrix (ecm)[1] of higher eukaryotes. These adhesins are collectively called microbial surface components recognizing adhesive matrix molecules (for review, see Ref. 2). One microbial surface component recognizing adhesive matrix molecule family comprises clumping factor A, which promotes adherence to fibrin and fibrinogen-coated surfaces (3) and the recently discovered clumping factor B, an isoform of clumping factor A (4). These proteins have in common (i) a short signal sequence, (ii) a fibrinogen-interactive A domain, (iii) an R domain consisting of numerous repeats of the dipeptide Ser-Asp, (iv) a W segment that helps span the cell wall, (v) an LP*X*TG motif, (vi) a hydrophobic membrane-spanning region, and (vii) a short, positively charged C terminus located in the cytoplasm (2). The Ser-Asp repeat is encoded by a characteristic 18-base pair DNA repeat, which was used as a probe in Southern hybridization to reveal genes specifying new members of the Sdr (SD repeat) protein family in *S. aureus* named SdrC, SdrD, and SdrE (43). The function of these Sdr proteins is not known, but it seems likely that they too mediate interactions of *S. aureus* with the ecm.

The new Sdr proteins contain, in addition to the above-mentioned domains, two, three, and five (for SdrC, SdrE, and SdrD, respectively) B-repeats of 110–113 residues inserted between the A and R regions (Fig. 1). The differing numbers of B-repeats in the three Sdr proteins suggest that they may serve as spacers to regulate the distance between the interactive A domain and the surface of the bacteria, although the B-repeats themselves may represent ecm binding sites. Each B-repeat contains three conserved stretches of 31 (C1), 32 (C2), and 25 (C3) residues with 36, 32, and 20%, respectively, sequence identity in the 10 B-repeats. C1 contains a 12-residue-long peptide corresponding to the loop of a canonical EF-hand motif (6). The EF-hand motif is a 29-residue-long, acidic helix-loop-helix that is always duplicated to form a paired folding unit (7). It is common to many intracellular Ca^{2+}-binding proteins, and its presence has recently been described in the extracellular proteins nucleobindin (8) and BM-40 (9). In addition, low-consensus EF-hands have been found in other extracellular proteins (10). It must be noted that well documented reports on prokaryotic proteins with EF-hand motifs are extremely rare (11): calerythrin, with three functional EF-hands, has been found in the genome of *Saccaropolyspora erythraea* (12), and a periplasmic D-galactose-binding protein with one unpaired EF-hand was found in *Escherichia coli*, and its three dimensional structure was determined (13). C2 and C3, the other conserved domains in the B-repeats, contain several D*X*(D/N) motifs and show homology to the putative Ca^{2+} binding sites in the β-propeller domain of integrin α4 subunit (14, 15). Recently we expressed in *E. coli* and purified the polypeptide segment of SdrD that encompasses the five B-repeats and which we will call B1–B5.[2] This protein segment undergoes large conformational changes with the addition of micromolar amounts of Ca^{2+}, suggesting that it contains high affinity Ca^{2+}-binding sites.

Here we provide a detailed description of the thermodynamic and kinetic parameters of the interaction of B1–B5 with Ca^{2+}, including the slow induction of 9–10 high affinity Ca^{2+}-binding sites. We describe the effect of Ca^{2+} binding on the secondary structure, on the microenvironment of the aromatic residues, and on the reactivity of the single thiol. From its hydrodynamic

* This work was supported by the Swiss National Science Foundation (to J.A.C. and I.D.); the King Gustav V 80th Birthday Foundation, the Swedish Medical Research Council, the Swedish Institute, and the Adlerbertska Foundation (to E.J.); and BioResearch Ireland, Forbairt, and The Wellcome Trust (to T.J.F. and D.O.). The costs of publication of this article were defrayed in part by the payment of page charges. This article must therefore be hereby marked "*advertisement*" in accordance with 18 U.S.C. Section 1734 solely to indicate this fact.

¶ To whom correspondence should be addressed: Dept. of Biochemistry, University of Geneva, 30 Quai Ernest-Ansermet, 1211 Geneva 4, Switzerland. Tel.: 41-22-702-6491; Fax: 041-22-702-6483; E-mail: jos.cox@biochem.unige.ch.

[1] The abbreviations used are: ecm, extracellular matrix; $[Ca^{2+}]_{0.5}$, calcium concentration at half-maximal change; CD, circular dichroism; PAGE, polyacrylamide gel electrophoresis.

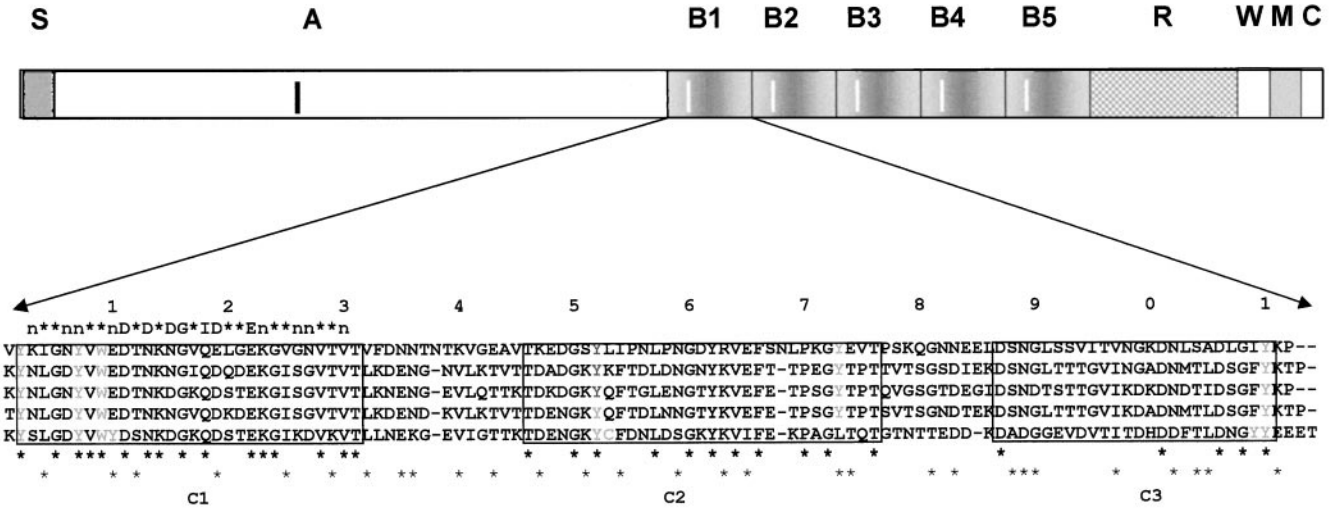

FIG. 1. *Top*, domain structure of SdrD. *A*, putative ecm binding segment with a TYTFTDYVD conserved motif (*vertical bar*); *B*, five B-repeats with the EF-hand loops (*white vertical bars*); *R*, 150 Ser-Asp residues; *W*, wall-spanning segment; *M*, membrane-spanning segment; *C*, cytoplasmic C-terminal end. *Bottom*, sequence of B1–B5 of SdrD. The *dashes* indicate deletions. The consensus sequence for a canonical EF-hand is taken from that of Kretsinger (6). The positions of Trp, Tyr, and Cys, residues relevant for this study, are also indicated. *Bold stars*, sequence identity in all five B-repeats; *thin stars*, sequence identity in four of the five B-repeats.

behavior we determined the shape and the geometric relation between the individual B-repeats.

MATERIALS AND METHODS

Protein Expression and Purification—Bacterial growth, protein expression in *E. coli*, and extraction of the recombinant protein segment were carried out as described elsewhere.[2] The B1–B5 protein was engineered to contain a hexahistidine tag in the N terminus. The tag was removed with the TAGZyme system (Unizyme Laboratories A/S, Hørsholm, Denmark) using histidine-tagged dipeptidyl aminopeptidase I to digest the histidine tag. Histidine-tagged dipeptidyl aminopeptidase I stops N-terminal to the dipeptide GS according to the manufacturer. Histidine-tagged dipeptidyl aminopeptidase I and the putative residual histidine-tagged B1–B5 were retained on a Ni^{2+} column. Further purification was carried out on a 3 × 15-cm column of Q-Sepharose fast flow equilibrated in 10 mM Tris-HCl, pH 7.5, 50 μM $CaCl_2$, which was eluted with a linear gradient of 0–0.4 M KCl. The purification was monitored by polyacrylamide electrophoresis in the presence of SDS. The final purity was shown by electrophoresis in 10% acrylamide rod gels in the presence and absence of SDS, both in the presence of 1 mM EGTA or Ca^{2+}.

Quaternary Structure Determination—Apparent molecular weights were determined by gel filtration on a 40 × 0.5-cm TSK column equilibrated in 50 mM Tris-HCl, pH 7.5, 150 mM KCl, and either 1 mM Ca^{2+} or 1 mM EGTA. Samples of 50 μg of protein were loaded. The Stokes radius (R_S) was estimated by comparison of the mobility of B1–B5 with that of a series of standard proteins (Bio-Rad standard).

To resolve the question of whether B1–B5 is oligomeric or monomeric under native conditions, it was submitted to native PAGE in gels of 5, 7.5, 10 and 12.5% acrylamide equilibrated in either 1 mM EGTA or 1 mM Ca^{2+} (16), together with the molecular mass standard proteins NSCP (20 kDa), bovine serum albumin monomer (68 kDa), and bovine serum albumin dimer (136 kDa). The mobilities (R_f) were measured, and the slopes of the linear plot, $\log R_f$ *versus* acrylamide percentage, were measured, yielding the retardation quotient for each protein. The Ferguson plot, retardation quotient *versus* molecular weight, allows evaluation of the native molecular mass of B1–B5, both in the presence and in the absence of Ca^{2+}.

Metal Removal—The proteins were precipitated with 3% trichloroacetic acid and then passed through a 40 × 1-cm Sephadex G-25 column equilibrated in 50 mM Tris-HCl, pH 7.5, 150 mM KCl (buffer A). Typically the contaminating Ca^{2+} represents <1.5% of the total binding capacity. Total Ca^{2+} and Mg^{2+} concentrations were determined with a Perkin-Elmer 2380 atomic absorption spectrophotometer. The protein concentration was determined from the ultraviolet absorption spectrum using the molar extinction coefficient $\epsilon_{278\ nm}$ = 68,200 M/cm. The coefficient was determined on a protein solution in 5 mM ammonium bicarbonate, the dry mass of which was subsequently determined after lyophilization and extensive drying over phosphorouspentoxide. It is close to the theoretical value of 68,130, based on the content of the Tyr, Trp, and Cys residues.

Cation Binding—Three methods for direct monitoring of Ca^{2+} binding to B1–B5 were used: equilibrium dialysis, flow dialysis, and fluorimetry using the Ca^{2+} indicators BTC and Mag-fura-2 (Molecular Probes, Eugene, OR). In equilibrium dialysis experiments (17) 500-μl samples of 10–50 μM protein in buffer A were dialyzed at 25 °C for 60 h (with one buffer change) against 100 ml of buffer A containing from 0.5 μM–1 mM free Ca^{2+}. At low free Ca^{2+}, solutions of 10 μM total Ca^{2+} were complemented with different concentrations of EGTA or nitrilotriacetic acid, and the precise $[Ca^{2+}]$ was calculated with the speciation program of Perrin and Sayce (18) using the complexation constants of Martell and Smith (19). Protein concentrations were determined spectrophotometrically, and the total inside and outside Ca^{2+} concentrations were determined by atomic absorption.

Flow dialysis in the absence or presence of 2 and 10 mM Mg^{2+} was carried out at 25 °C in buffer A with protein concentrations of 20–30 μM according to the modified method of Colowick and Womack (20). Treatment of the raw data and evaluation of the metal binding parameters were as described by Cox (21).

BTC and Mag-fura-2 fluorimetry was adapted from a method previously described (22): to a solution of 15 μM metal-free B1–B2 and 3 μM indicator, 20 μM increments of Ca^{2+} were added, and the fluorescence excitation spectra were monitored after each addition with both slits set at 5 nm. For BTC, fluorescence intensities at 401 (increasing) and 469 nm (decreasing) were ratioed with respect to those at the isosbestic point at 433 nm to eliminate interferences or lamp intensity changes. Corresponding data extractions for Mag-fura were at 332 (increasing), 352 (isosbestic point), and 385 nm (decreasing), respectively. The signal changes were normalized from 0 (nominally zero $[Ca^{2+}]$) to +1 (saturating $[Ca^{2+}]$), yielding ΔS_{332} and ΔS_{385}, which were subsequently averaged to yield ΔS_i. The concentration of free Ca^{2+} was then calculated by intrapolation of these ΔS_i values at each Ca^{2+} increment to the Ca^{2+}-binding isotherm of BTC or Mag-fura-2. The latter was estimated independently under our working conditions and yielded affinity constants of 1.4×10^5 and 1.8×10^4 M for BTC and Mag-fura-2, respectively. Protein-bound Ca^{2+} was calculated by subtracting the free $[Ca^{2+}]$ from the total amount of added Ca^{2+} plus the initial contamination, determined by atomic absorption.

Kinetics of Ca^{2+} Binding Followed with BTC—The kinetics of Ca^{2+} binding to B1–B5 was monitored fluorimetrically during a Ca^{2+} titration of 17 μM B1–B5 in the presence of 3 μM BTC. Excitation was at either side of the isosbestic point (323 and 382 nm). It was checked that the fluorescence changes of BTC alone with the addition of Ca^{2+} or EGTA were instantaneous in our experimental setup. A speciation program (18) was used to calculate the concentrations of the different protein-Ca^{2+} complexes from the added concentrations of protein, indicator, and Ca^{2+} and from their affinity constants.

Secondary Structure Monitored by Circular Dichroism—Circular di-

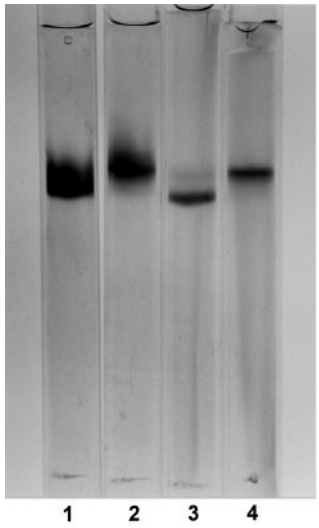

FIG. 2. **Polyacrylamide gel electrophoresis of purified B1–B5.** PAGE was performed in the absence (*lanes 1* and *2*) and presence (*lanes 3* and *4*) of SDS and in the presence of 1 mM EGTA (*lanes 1* and *3*) or 1 mM Ca^{2+} (*lanes 2* and *4*).

chroism (CD) spectra were acquired with a Jasco J-715 spectropolarimeter in 10 mM Tris-HCl buffer, pH 7.5. Far UV CD was done on solutions of 0.25 mg/ml protein in a cell of 1-mm optical path. Near UV CD was on a 1.8 mg/ml protein solution in a 1-cm cell. Ellipticities were normalized to residue concentration using the relationship: $\theta_{MRW} = \theta_o M_r / lc$, where θ_o is the observed ellipticity in millidegrees, M_r is the average molecular weight of an amino acid in the polypeptide, l is the path length in mm, and c is the protein concentration in mg/ml.

Conformational Changes Monitored by Trp Fluorescence—Emission fluorescence spectra were taken with a Perkin-Elmer LS-5B spectrofluorimeter. The measurements were carried out on 2 μM metal-free B1–B5 in buffer A at room temperature with excitation wavelength at 278 nm and slits of 5 nm. 25 μM EGTA or 5 mM $CaCl_2$, or 50 mM $MgCl_2$ or 4 M guanidine-HCl was added to obtain the metal-free Ca^{2+} or Mg^{2+} forms, respectively. The kinetics of Trp fluorescence change was measured at 325 nm, and the data were analyzed with the Guggenheim equation for first order reactions.

Protein Reduction and Thiol Reactivity—The thiol reactivity was assayed after overnight incubation with 100 mM dithiotreitol, pH 8.5, followed by desalting on a Sephadex G-25 column equilibrated in nitrogen-saturated buffer A. The thiol reactivity was monitored by measuring the kinetics of the reduction of Ellman's reagent by spectrophotometry at 412 nm according to the method of Riddles *et al.* (23).

RESULTS

Protein Expression and Purification—After proteolytic removal of the hexahistidine-tag, the protein had one short additional segment, SKLN, at the C terminus. In the Q-Sepharose chromatography pure B1–B5 eluted with a profile of at least three overlapping peaks at conductivities between 5 and 16 mmho (~0.1 and 0.3 M KCl) but separated from proteolytically degraded B1–B5, which eluted at 1–3 and >17 mmho, respectively. The protein was pure, as judged from PAGE in the presence and absence of SDS, both in the presence of 1 mM EGTA or Ca^{2+} (Fig. 2). In both conditions metal-free B1–B2 showed a slightly higher mobility than the Ca^{2+} form. During TSK gel filtration experiments in the presence of 1 mM Ca^{2+} or EGTA B1–B5 eluted as a single symmetrical peak (data not shown). The conformational heterogeneity of electrophoretically pure B1–B5 during Q-Sepharose chromatography is not attributable to differences in the amount of protein-bound Ca^{2+} as measured by flame spectrophotometry. A very similar elution profile was observed when the chromatography was done in the presence of EGTA instead of Ca^{2+}.

Direct Ion Binding Studies: Slow Induction of Additional High Affinity Ca^{2+} Binding Sites—Equilibrium gel filtration experiments at low (10 mM Tris-HCl, pH 7.5) as well as moderately high ionic strength (50 mM Tris-HCl, pH 7.5, 150 mM KCl) and a free Ca^{2+} concentration of 40–60 μM showed that B1–B5 binds 14–15 mol of Ca^{2+}/mol, which seems to be a very good estimation of the total capacity. Equilibrium dialysis at 25 °C in buffer A yielded the binding isotherm depicted in Fig. 3 (*triangles*). B1–B5 binds 14 Ca^{2+} ions with a mean dissociation constant ($[Ca^{2+}]_{0.5}$) of 4 μM and a Hill coefficient of 1.08. The data suggest that each B-repeat is an autonomous unit with three high affinity Ca^{2+}-binding sites. Surprisingly the isotherm obtained by flow dialysis at 25 °C in buffer A (Fig. 3, *open circles, rectangles*, and *hexagons*) is biphasic, displaying one set of five sites with a $[Ca^{2+}]_{0.5}$ of 3 μM and Hill coefficient of 1.45 and a second set of 10 sites with a $[Ca^{2+}]_{0.5}$ of 190 μM and a Hill coefficient of 1.08. The presence of 2 or 10 mM Mg^{2+} concentrations has no effect on the isotherm, indicating that all of the sites are Ca^{2+}-specific. This discrepancy between the two methods, which was never observed for intracellular Ca^{2+}-binding proteins, incited us to use a third method for measuring Ca^{2+}-binding isotherms: the fluorimetric titration in the presence of the Ca^{2+} indicators BTC and Mag-fura-2. The two indicators, which are maximally active at different free Ca^{2+} concentrations (different dissociation constants), cover precisely the zone of interest. Fig. 3 (*stars* for Mag-fura-2, *crosses* for BTC) shows that the isotherm obtained with this method is very similar to the one obtained with equilibrium dialysis. Thus B1–B5 contains two types of sites: one class of five sites displaying high affinity when monitored with all three methods and one class of 9–10 sites, which display a high affinity in the equilibrium dialysis and fluorimetric method but a low affinity when monitored with the flow dialysis method.

These discrepant results can be explained in two ways: (i) the instantaneous binding of the first five Ca^{2+} ions involves a slow induction of 10 additional high-affinity Ca^{2+}-binding sites, and therefore the flow dialysis method might be too fast for the protein to reach a stable equilibrium at each increment, and the induced sites are perceived as low affinity sites, or (ii) the affinity of the second class of Ca^{2+}-binding site is decreased by hydrodynamic shear induced by rapid stirring of the protein solution, operative in the flow dialysis method only. One argument against the first working hypothesis was that a flow dialysis experiment in which both the addition of increments and the perfusion rate were slowed down 3-fold yielded exactly the same data as in the usual 40-min-long flow experiments (Fig. 3, *stars*). In favor of the hypothesis of slow induction of high-affinity sites is the finding that during the titration experiment with BTC it was noted that stabilization of the fluorescence signals occurred only after a few minutes. Therefore a Ca^{2+} titration was carried out on B1–B5 in the presence of BTC while monitoring the fluorescence change of the indicator at 469 nm. Because BTC displays fast Ca^{2+} binding kinetics, the slow induction of high-affinity Ca^{2+}-binding sites on B1–B5 should lead to an equally slow release of Ca^{2+} from the indicator, especially because the affinity of B1–B5 for Ca^{2+} is 2-fold higher than that of BTC. Fig. 4*A* shows that Ca^{2+} increments lead to an instantaneous fluorescence decrease (binding of Ca^{2+} to BTC) followed by a slow increase (dissociation of Ca^{2+} from BTC), as expected in the model of site induction. Similar kinetic experiments monitored over longer time spans for each increment (Fig. 4*B*) revealed that each of the slow steps follows first order kinetics with $t_{1/2}$ values increasing from 0.3 to 12 min at higher Ca^{2+} increments. For example, after addition of 25 or 50 μM Ca^{2+} to a 10 μM solution of B1–B5, 4 and 11 μM Ca^{2+} dissociates slowly from BTC with $t_{1/2}$ values of 1.5 and 5 min, respectively. Because Ca^{2+} not only dissociates from BTC but also is redistributed from the five fast high affinity sites to the induced ones, these amplitudes of the signal change are

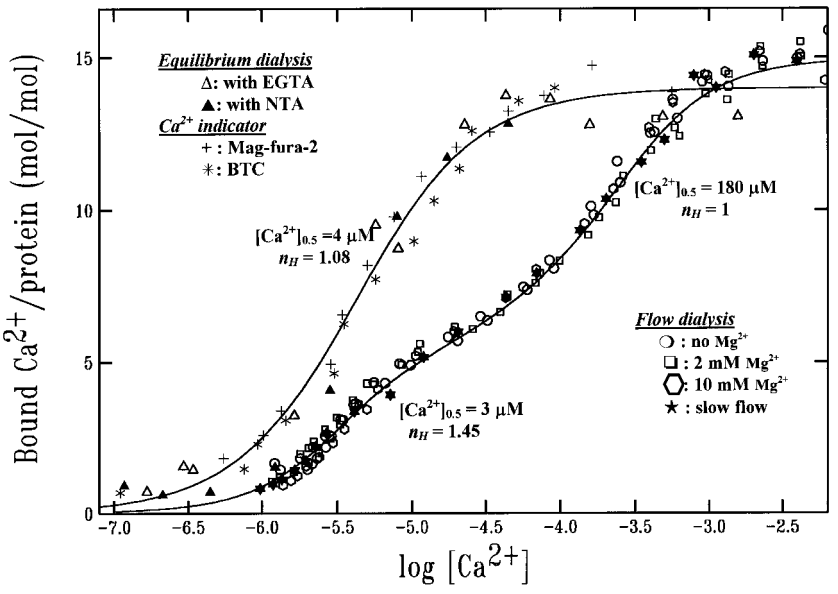

FIG. 3. **Ca^{2+} binding to B1–B5 of SdrD at 25 °C in buffer A.** Equilibrium dialysis in the presence of nitrilotriacetic acid (NTA) (*open triangle*) or EGTA (*closed triangle*), fluorimetry with the Ca^{2+} indicators BTC (+) and Mag-fura-2 (✳), and flow dialysis in the absence (*circles*) or presence of 2 mM (*rectangle*) or 10 mM (*hexagon*) Mg^{2+} were performed. One flow dialysis experiment was performed at a 3-fold slower pace, *i.e.* 6 min/increment (*stars*). The isotherms connecting the symbols were generated using the binding parameters indicated under "Results."

sufficient to explain the discrepancy between the equilibrium and flow dialysis experiments. The dependence of the rate of site induction on the total Ca^{2+} concentrations is at present not understood but may be related to either local or global conformational changes in B1–B5. To test the second hypothesis of a shear-induced decrease of the Ca^{2+} affinity in the flow dialysis experiments, a BTC-monitored titration experiment was carried out in a magnetically stirred cuvette at same speed as during flow dialysis, but with frequent arrests of the stirrer. Fig. 4*B* shows that the starts and stops did not noticeably affect the fluorescence changes. In conclusion, our fluorescence data presented in Fig. 4 suggest that the induction of high affinity sites explains the discrepancy between the flow and equilibrium dialysis experiments presented in Fig. 3.

The Quaternary Structure and Shape of B1–B5—The theoretical molecular mass of B1–B5, deduced from the sequence, is 64.8 kDa. However, on a TSK gel filtration column equilibrated in buffer A containing 1 mM EGTA or 1 mM Ca^{2+}, it eluted with apparent molecular masses of 320 and 250 kDa, respectively. Thus, either native B1–B5 is an oligomer or it has an elongated shape. To distinguish between these two possibilities, B1–B5 was submitted to PAGE in the absence of SDS but at different acrylamide concentrations (10). This method led to the estimation of a molecular mass of 64 ± 6 kDa for both the Ca^{2+}-saturated and metal-free forms (data not shown). Interestingly, in these "native" gels metal-free B1–B5 migrates 1.3-fold faster than the Ca^{2+} form, but the molecular weight evaluation yields the same value. These data indicate that in native conditions B1–B5 is a monomer but has an elongated shape either because of the absence of any structure (natively unfolded), as for NACP protein (24), or because it has the shape of a rigid rod, as in the case of the extracellular domain of E-cadherin (25). Optical methods probing the degree of folding allowed us to discriminate between these two possibilities (next section).

Secondary Structure Probed by Circular Dichroism—Fig. 5*A* shows the far UV CD spectra of B1–B5 measured in the presence of Ca^{2+} or EGTA at 25 and 85 °C. In general the ellipticities are low, which accentuates the contributions of aromatic residues in the far UV region (26). The spectra of the heated samples display a minimum at 201 nm, and their shape is as expected for fully denatured proteins. Because, except for a blue shift of the minimum to 197 nm, the spectrum of metal-free B1–B5 at 25 °C is very similar, this form must contain very little organized secondary structure. In contrast, the Ca^{2+}-loaded protein shows discrete peaks: one positive peak at 228 nm, which may be attributable to aromatic residues (26), and two negative peaks at 215 and 195 nm. All of the spectral changes are fully reversible when the protein is cooled down from 85 to 25 °C. The cation-dependent ellipticity change was completed within the dead time (28 s) of the experiment (data not shown).

Proteins containing Trp, Tyr, and Phe usually have very complex near UV CD spectra (27), however, those of B1–B5 showed only one narrow negative peak at 280–283 nm (Fig. 5*B*). Their nearly symmetric shape and surprising simplicity suggest that Trp and Phe do not contribute to the spectrum, in other words, that they are not located in an in an asymmetric microenvironment. The Tyr residues 2, 7, 52, 73, and 100 (Fig. 1) are very well conserved in all of the B-repeats, and the spectra suggest that the rotation of several of these is restricted, as was also found in the case of wild-type and deletion mutants of interleukin-6 (28, 29) and in the synthetic $(Tyr\text{-}Ala\text{-}Glu)_n$ polypeptide (30). Removal of Ca^{2+} changed the intensity of ellipticity only slightly, with a 2-nm blue shift, indicating that microenvironment of the Tyr residues in apoB1–B5 is asymmetric and therefore structured.

Trp Fluorescence of B1–B5—B1–B5 contains five well conserved Trp residues, one in position 9 of each B-repeat (Fig. 1). Fig. 6 shows the emission spectra of a 1 μM solution of B1–B5 after excitation at 278 nm. The spectrum of the metal-free protein is quite similar to that of the guanidine-HCl-denatured form, although its intensity is 20% higher, and the maximum blue shifted by 5 nm. The Ca^{2+}-saturated protein shows a 2.5-fold higher fluorescence intensity and a blue shift from 345 to 323 nm compared with the metal-free state, suggesting that with Ca^{2+} binding a well organized hydrophobic core is formed around the Trp residue (31). Mg^{2+} had no effect (data not shown), which confirms the conclusion from flow dialysis that all of the sites are Ca^{2+}-specific. By monitoring the kinetics of the Trp fluorescence change at 325 nm, we observed that Ca^{2+} binding strongly stabilizes B1–B5 against denaturation by urea and guanidine-HCl. For example, after addition of 4 and 6 M guanidine-HCl, first order kinetics were observed with $t_{1/2}$ values of 12 and 4.8 min, respectively. In 7.5 M urea the $t_{1/2}$ value was 39 min, and in 4 M urea no significant change was observed. In conclusion, the Ca^{2+} form of B1–B5 is remarkably stable, as has been reported for several β-sheet-rich proteins.

During the fluorimetric experiments it appeared that the

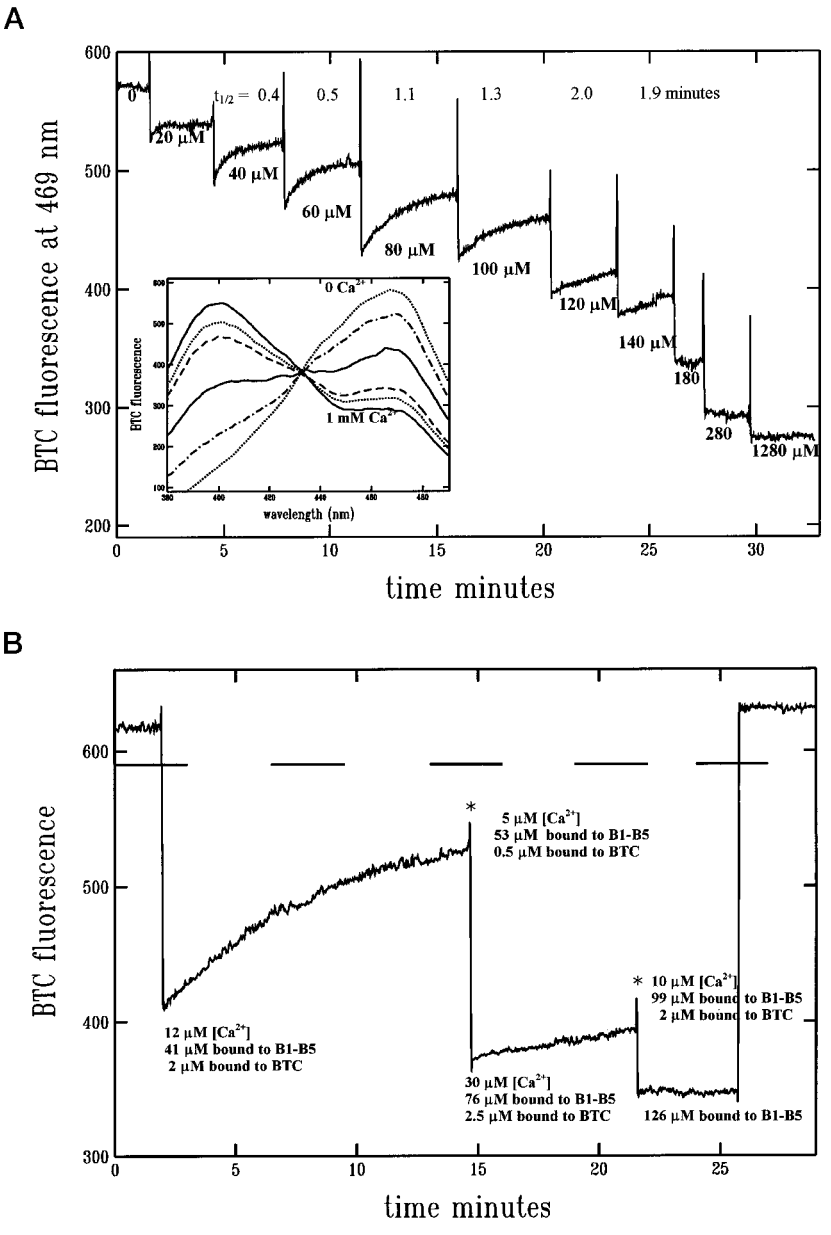

FIG. 4. **Regulation of the number of high-affinity sites in B1–B5.** *A*, kinetics of Ca^{2+} binding to induced high-affinity sites in B1–B5 (17 μM) monitored by the fluorescence decrease of the Ca^{2+} indicator BTC (3 μM). Increments of Ca^{2+} were added to obtain the indicated final Ca^{2+} concentrations. Ca^{2+} dissociation from the indicator followed first order kinetics with $t_{1/2}$ values indicated for the most relevant steps. *Inset*, representative excitation spectra of BTC during the titration of the mixture of 3 μM BTC and 17 μM B1–B5 with Ca^{2+}. *B*, effect of shear on the affinity. The experimental conditions are as in Fig. 5*A*, except for intermittent stirring in a 3-ml cuvette (*horizontal bars* correspond to periods of stirring). Three increments of 55 μM Ca^{2+} were added at 1.5, 14.8, and 21 min, followed by addition of 1 mM EGTA at 26 min. The kinetics of the signal change after the first two Ca^{2+} increments were evaluated with the Gugenheim equation and yielded $t_{1/2}$ values of 1.5 and 12 min, respectively, and extrapolated maxima indicated by the two *stars*. The values at each extreme indicate the free and B1–B5- and BTC-bound Ca^{2+} concentrations, respectively, as evaluated from the signal changes.

binding of Ca^{2+} caused slow conformational changes. Fig. 6, *inset*, shows that the addition of Ca^{2+} to metal-free B1–B5 leads to a biphasic change in the Trp fluorescence: one very fast step with an amplitude of 33%, followed by a slow step of 67% amplitude that takes >15 min and follows strict first order kinetics with an estimated $t_{1/2}$ of 3.1 ± 0.3 min. Addition of EGTA to the Ca^{2+}-saturated protein caused an instantaneous fall to the fluorescence level of the metal-free protein. The kinetics of the slow phase was not Ca^{2+}-dependent between 100 μM and 2.5 mM, suggesting that this phase does not represent the binding process itself but a subsequent slow conformational change in Trp environment. As expected, the kinetics is also independent of Mg^{2+}. Kinetic experiments (Fig. 7) in which subsaturating concentrations of Ca^{2+} were added stepwise to 4.9 μM B1–B5 protein revealed that the onset of the slow reaction is strictly dependent on the amount of Ca^{2+} bound to the protein; the small initial Ca^{2+} increments promoted the fast fluorescence increase but not the subsequent slow phase. Only after the binding of 5–8 mol of Ca^{2+}/mol of protein did the slow fluorescence increase start to take place, and this was independent of the protein concentration between 0.5 and 4 μM.

Cys Reduction and Thiol Reactivity—B1–B5 contains one single Cys residue in position 51 of the fifth B-repeat (Fig. 1). After overnight reduction with 100 mM dithiotreitol at 4 °C, excess of reagent was removed by Sephadex G-25 chromatography in degassed and then nitrogen-saturated buffer. When assayed with the 5,5′dithiobis(2-nitrobenzoic acid) reagent, B1–B5 contains 1.05 mol of free accessible thiol. This thiol reacted instantaneously in the presence of 4 M guanidine-HCl, rapidly in the native apo state ($t_{1/2}$ = 13 s), and slowly in the Ca^{2+} state ($t_{1/2}$ = 86 s).

DISCUSSION

$[Ca^{2+}]_o$ exerts biological effects on eukaryotic extracellular Ca^{2+}-binding proteins with sensitivities in the millimolar range. These multidomain proteins possess well defined Ca^{2+} binding units (for review, see Ref. 10). Examples are the EF-hand in BM-40, the E-cadherin repeat in the homonymous protein, the epidermal growth factor-like fold in many ecm proteins, best exemplified by fibrillin, the E-selectin fold, and the GLA motif in blood-coagulating proteins. Functionally these motifs are involved either in rigidification and orientation of a part of the protein or in the binding of the protein to

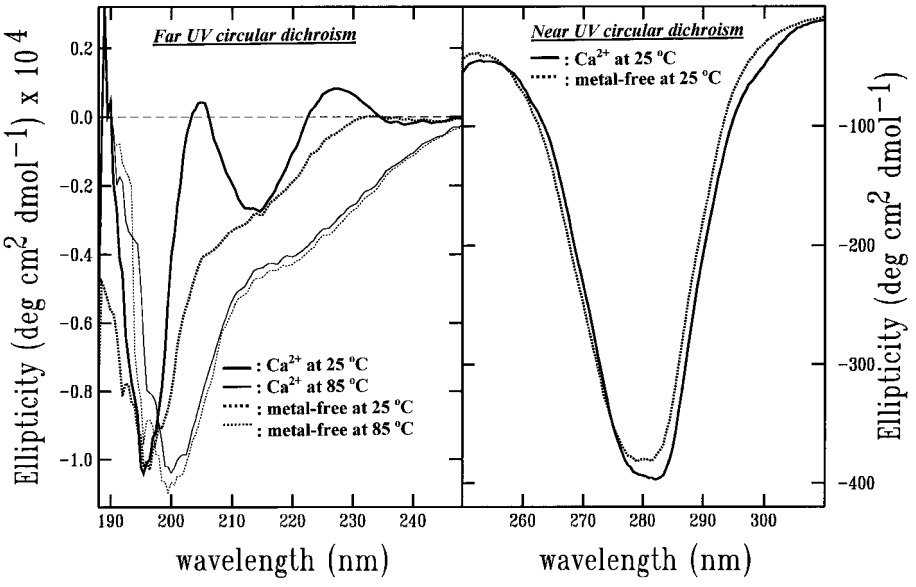

FIG. 5. **Far UV (*A*) and near UV (*B*) CD spectra of B1–B5 of SdrD.** Spectra were recorded at 25 and 85 °C on 0.25 (*A*) or 1.5 (*B*) mg/ml protein in 5 mM Tris-HCl buffer, pH 7.5, in the metal-free state (*dotted lines*) or in the presence of 5 mM Ca^{2+} (*solid lines*).

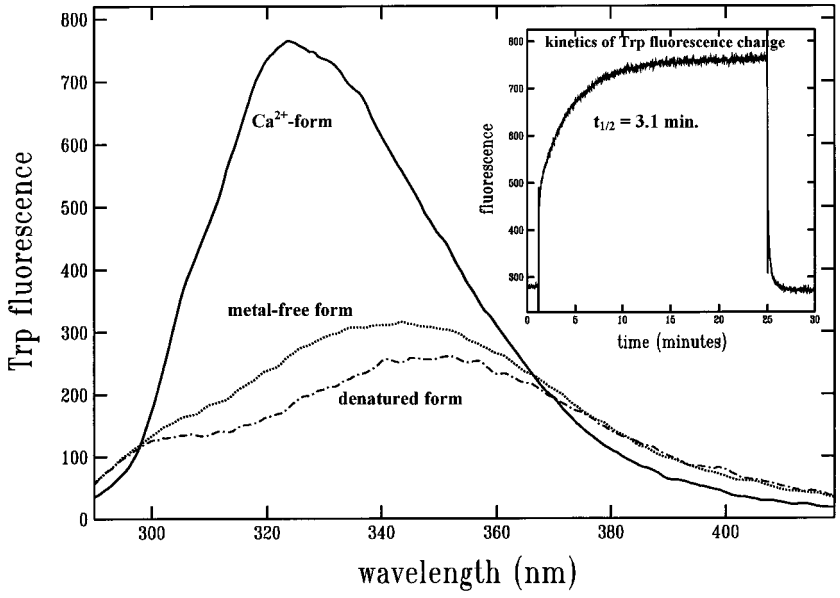

FIG. 6. **Fluorescence spectra of B1–B5.** Spectra were recorded at room temperature in buffer A on 1 μM protein in the metal-free state (*dotted lines*), in the presence of 5 mM Ca^{2+} (*solid lines*), or in the presence of 4 M guanidine-HCl (*dashed* and *dotted lines*). *Inset*, kinetics of the fluorescence change after addition of 2 mM Ca^{2+} to metal-free protein, as monitored at 325 nm.

ecm proteins, carbohydrates, or lipid membranes. Recently we showed that the Sdr cell surface protein family of the bacterium *S. aureus* contains repeats that may represent a new high affinity Ca^{2+} binding motif.[2] In this study we quantified the interaction of Ca^{2+} with B1–B5, a segment that represents the five repeats of SdrD.

Two different direct binding methods, *i.e.* equilibrium dialysis and fluorimetry with Ca^{2+} indicators of different affinity, showed that B1–B5 binds a total of 14–15 Ca^{2+} with a mean dissociation constant of 4 μM. With a third method, namely flow dialysis, we persistently found that there are two class of binding sites: class I comprises a set of five with high affinity; class II comprises a set of 9–10 sites of low affinity. Thus, the class II sites display a low affinity in the rather fast flow dialysis method (40 min for a whole titration) and a high affinity in the slow equilibrium dialysis technique (48 h of dialysis). One explanation for this unusual behavior is that at the start of the flow dialysis metal-free B1–B5 displays only the 5 class I high-affinity sites, and after Ca^{2+} binding to these sites 10 additional high affinity sites are induced, but at such a slow pace that in the flow dialysis the latter are perceived as low affinity sites. This working hypothesis could partially be confirmed by kinetic experiments with the fast reacting fluorescent Ca^{2+} indicator BTC. In a titration of apo B1–B5 we observed that increments of Ca^{2+} are rapidly bound to the indicator and to class I sites and then are slowly redistributed (with dissociation of Ca^{2+} from BTC) to the induced class II sites. The amplitudes of the Ca^{2+} fluxes are compatible with this working hypothesis, but the kinetics of induction as monitored with BTC are too fast to explain fully the data of the flow dialysis. It is at present also not clear why the rate of induction is inversely proportional to the amount of total Ca^{2+} in each increment. Besides Ca^{2+}-binding site induction, other phenomena may be partially responsible for the discrepancy between the two methods, but the hypothesis of a modulating effect of hydrodynamic shear on the affinity of the class II sites could be discarded.

Calibrated molecular sieving and PAGE in the absence of SDS together indicate that Ca^{2+}-bound B1–B5 is monomeric but displays an elongated shape. This is reminiscent of the E-cadherin homoassociation domain, which, as with B1–B5, contains five repeats of 110–115 amino acids each and numerous Ca^{2+}-binding sites. In E-cadherin each repeat, called cadherin fold, represents a cylindrically shaped folding unit (25 ×

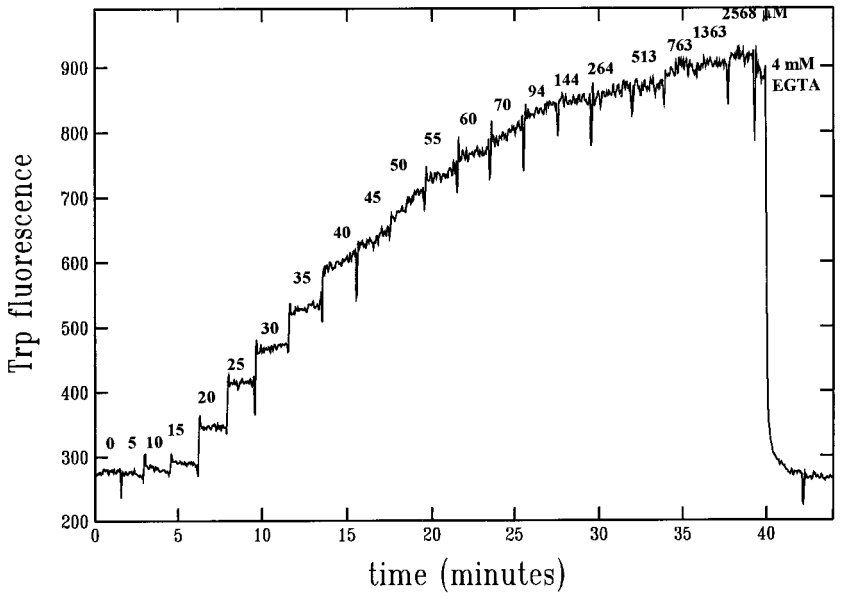

FIG. 7. **Kinetics of the Trp fluorescence changes on the Ca^{2+} titration of 4.9 μM B1–B5.** Increments of Ca^{2+} were added to obtain the indicated final Ca^{2+} concentrations. At 40 min EGTA was added to a final concentration of 4 mM.

25 × 45 Å) composed of seven β-strands (32). The Ca^{2+}-binding sites are located in the joints between the cadherin folds. Ca^{2+} binding leads to a stiffening of the joints with a strong restriction of the flexibility between adjacent cadherin folds. It is tempting to propose this elegant "elbow rigidification" model in the case of B1–B5, but some basic differences exist between the two pentamers. One argument against a structural homology is that our electron microscopic studies on B1–B5 failed[3] to show any of the well-organized repeated entities that were observed in the case of E-cadherins (33, 34).

In light of the pentameric symmetry, it is tempting to assume that each B-repeat contains one class I site and two class II sites. This hypothesis is strengthened by preliminary experiments on a single B-repeat[4] and by the sequence conservation in each B-repeat. The five class I sites may be located in the N-terminal EF-hand loop of the C1 segment, which is very well conserved in each B-repeat. The 10 class II sites may be located in the C2 and C3 stretches, which are rich in D*X*(D/N) sequences. For a more educated guess one needs to know the three-dimensional structure of a B-repeat. The unusual far UV CD spectrum of the Ca^{2+} form of B1–B5 resembles that of the central and the heparin-binding segments of fibronectin (35, 36), which are essentially composed of 90-residue-long type II motifs. The content of the antiparallel β-sheet, the only element of secondary structure, was estimated to be 30–35%, although dominant Tyr effects may have altered the prediction (37). The three-dimensional solution structure of the 10th fibronectin type III motif (38) shows that seven β-strands form two antiparallel β-sheets, packed against each other (as in the Ig fold). This motif possesses the same fold as glycoprotein CD4, D2 of chaperone protein papD, and the extracellular region of human growth hormone receptor, but there is no significant sequence similarity between these proteins. Therefore we did not attempt a sequence alignment with B1–B5.

But neither fibronectin nor E-cadherin unfold as does metal-free B1–B5. Metal-free B1–B5 displays a "natively unfolded state" according to the concept of Mandelkow taken up by Weinreb *et al.,* (24) and Matsubara *et al.,* (39). It contains little secondary structure and nearly no hydrophobic core. Nevertheless, it differs from the completely unfolded protein by the presence of some β-turns, the reduced reactivity of the thiol, an asymmetric environment of the Tyr residues, as interferred from the near UV CD (Fig. 5*B*) and difference spectra (data not shown) and by the strong interaction with bis-4,4′-dianilino-1,1′-bisnaphthyl-5,5′-disulfonate.[2] It most likely corresponds to an early intermediate with collapsed hydrophobic residues, described by Nath and Udgaonkar (40). The partial collapse of hydrophobic residues, especially of Tyr residues, may explain why it does not aggregate. Proteins with this particular structure are reported to facilitate protein-protein interactions (24), but the observed high affinity for Ca^{2+} casts doubts that this metal-free conformation can occur *in vivo*.

For several reasons it is very unlikely that the EF-hand in the C1 region of these extracellular Sdr proteins has the conformation of the EF-hands in intracellular proteins and in the extracellular BM-40. First, B1–B5 does not possess a significant amount of α-helix needed to form the flanking α-helices of the canonical EF-hand. Second, metal-free B1–B5 is strongly destabilized, which is usually not the case in EF-hand proteins. Third, the comparison of the sequences of the C1 region in all of the B-repeats shows the following anomalies: (i) the Ile or Leu in the position between –Tyr and –*X* (Fig. 1), which is strongly conserved in all functional EF-hands (41, 42), is replaced by a polar Gln in all the B-repeats; (ii) the segments flanking the Ca^{2+} binding loop, which are α-helical in functional EF-hands, are in B1–B5 rich in α-helix breaking Pro and Gly residues; and (iii) their insertion on the loop does not involve the usual hydrophobic residues. So the structure of the Ca^{2+}-bound B-repeat poses an important question mark, and resolution of the three-dimensional structure by NMR or crystallography is eagerly awaited.

Apart from the problem of global shape of B1–B5 and the structure of each B-repeat, there is the question of why the affinities are so high in this protein, *i.e.* 20–200 times higher than in nearly all the other extracellular Ca^{2+} binding motifs. For a long time the $[Ca^{2+}]_o$, was thought to be constant, and, indeed, in blood it is stringently regulated to 1.1–1.3 mM by a homeostatic circuit, and deviations immediately lead to severe pathology. But recently it was reported that in the extracellular space $[Ca^{2+}]_o$ can vary by a factor of 10 and can control cell differentiation and tissue development (for review, see Ref. 5). It is thus likely that the always Ca^{2+}-loaded class I sites *in vivo* promote structural stability, whereas the class II sites may be under active control of extracellular Ca^{2+} homeostasis.

[3] I. Durussel and J. A. Cox, unpublished data.
[4] E. Josefsson, D. O'Connell, T. J. Foster, I. Durussel, and J. A. Cox, unpublished data.

In summary, the unusual high affinity of five sites for Ca^{2+}, the induction of additional Ca^{2+}-binding sites, the unusual CD spectra, and the greatly unfolded state of the metal-free form indicate that this B1–B5 repeat is a unique and new motif among extracellular Ca^{2+} binding motifs. The fact that it contains a nearly canonical EF-hand loop, but very likely not the EF-hand configuration as defined by Kretsinger (6), adds to the enigma of this protein family. Detailed structural studies on single and twin B-repeats are in progress to solve some of the numerous questions remaining.

REFERENCES

1. Projan, S. J. & Novick, R. P. (1997) in *The Staphylococci in Human Disease* (Crossley, K. B., and Archer, G., eds) pp. 55–81, Churchill Livingstone, New York
2. Foster, T. J., Hartford, O. & O'Connell, D. (1997) in *Molecular Aspects of Host-Pathogen Interaction* (McCrae, M. A., Saunders, J. R., Smyth, C. J., and Stow, N. D., eds) Society for General Microbiology, Symposium 55, pp. 67–94, Cambridge University Press, Cambridge, UK
3. McDevitt, D, Francois, P., Vaudaux, P. & Foster, T. J. (1994) *Mol. Microbiol.* **11,** 237–248
4. Ní Eidhin, D., Perkins, S., Francois, P., Vaudoux, P., Höök, M. & Foster, T. J. (1998) *Mol. Microbiol.* **29,** in press
5. Brown, E. M., Vassilev, P. M. & Hebert, S. C. (1995) *Cell* **83,** 679–682
6. Krestinger, R. H. (1987) *Cold Spring Harbor Symp. Quant. Biol.* **52,** 499–510
7. Shaw, G., Hodges, R. S. & Sykes, B. D. (1990) *Science* **249,** 280–283
8. Wendel, M., Sommarin, Y., Bergman, T. & Heinegard, D. (1995) *J. Biol. Chem.* **270,** 6125–6133
9. Hohenester, E., Maurer, P., Hohenadl, C., Timpl, R., Jansonius, J. N. & Engel, J. (1996) *Nat. Struct. Biol.* **3,** 67–73
10. Maurer, P., Hohenester, E. & Engel, J. (1996) *Curr. Opin. Cell Biol.* **8,** 609–617
11. Cox, J. A. (1996) in *Guidebook to the Calcium Binding Proteins* (Celio, M., ed) pp. 58–62, Oxford University Press, New York
12. Swann, D. G., Hale, R. S., Dhillon, D. & Leadlay, P. F. (1987) *Nature* **329,** 84–85
13. Vyas, N. K., Vyas, M. N. & Quiocho, F. A. (1987) *Nature* **327,** 635–638
14. Springer, T. A. (1997) *Proc. Natl. Acad. Sci U. S. A.* **94,** 65–72
15. Oxvic, C. & Springer, T. A. (1998) *Proc. Natl. Acad. Sci. U. S. A.* **95,** 4870–4875
16. Hames, B. D. (1990) in *Gel Electrophoresis of Proteins* (Hammes, B. D., and Rickwood, D., eds) pp. 12–18, Oxford University Press, New York
17. Wnuk, W., Cox, J. A., Kohler, L. G. & Stein, E. A. (1979) *J. Biol. Chem.* **254,** 5284–5289
18. Perrin, D. D. & Sayce, I. G. (1967) *Talanta* **14,** 833–842
19. Martell, A. E. & Smith, R. M. (1964) *Critical Stability Constants*, Vol. 1, Plenum Press, New York
20. Colowick, S. P. & Womack, F. C. (1969) *J. Biol. Chem.* **244,** 774–777
21. Cox, J. A. (1996) in *Guidebook to the Calcium Binding Proteins* (Celio, M., ed) pp. 1–44, Oxford University Press, New York
22. Eberhard, M. & Erne, P. (1994) *Eur. J. Biochem.* **222,** 21–26
23. Riddles, P. W., Blakeley, R. L. & Zerner, B. (1983) *Methods Enzymol.* **91,** 49–60
24. Weinreb, P. H., Zhen, W., Poon, A. W., Conway, K. A. & Lansbury, P. T. (1996) *Biochemistry* **35,** 13709–13715
25. Nagar, B., Overduin, M., Ikura, M. & Rini, J. M. (1996) *Nature* **380,** 360–364
26. Woody, R. W. (1994) in *Circular Dichroism. Principles and Applications* (Nakanishi, K., Berova, N., and Woody, R. W., eds) pp. 473–496, VCH Publishers, New York
27. Strickland, D. H. (1974) *CRC Crit. Rev. Biochem.* **2,** 113–175
28. Ward, L. D., Zhang, J. G., Checkley, G., Preston, B. & Simpson, R. J. (1993) *Protein Sci.* **2,** 1291–1300
29. De Filippis, V., Polverino de Laureto, P., Toniutti, N. & Fontana, A. (1996) *Biochemistry* **35,** 11503–11511
30. Schechter, B., Schechter, I., Rachamandran, J., Conway-Jacobs, A., Sela, M. (1971) *Eur. J. Biochem.* **20,** 301–308
31. Lakowicz, J. R. (1983) in *Principles of Fluorescence Spectroscopy*, Plenum Press, New York
32. Shapiro, L., Fannon, A. M., Kwong, P. D., Thomson, A., Lehmann, M. S., Grübel, G., Legrand, J.-F., Als-Nielsen, J., Colman, D. R. & Hendrickson, W. A. (1995) *Nature* **374,** 327–337
33. Pokutta, S., Herrenknecht, K., Kemler, R. & Engel, K. (1994) *Eur. J. Biochem.* **223,** 1019–1026
34. Alattia, J.-R., Ames, J. B., Porumb, T., Tong, K. I., Heng, Y., Ottensmeyer, P., Kay, C. M. & Ikura, M. (1997) *FEBS Lett.* **417,** 405–408
35. Venyaminov, S. Y., Metsis, M. L., Chernousov, M. A. & Koteliansky, V. E. (1983) *Eur. J. Biochem.* **135,** 485–489
36. Odermatt, E., Engel, J., Richter, H. & Hörmann H. (1983) *J. Mol. Biol.* **159,** 109–123
37. Stevens, E. S., Morris, E. R., Charlton, J. A. & Rees, D. A. (1987) *J. Mol. Biol.* **197,** 743–745
38. Main, A. L., Harvey, T. S., Baron, M., Boyd, J. & Campbell, I. D. (1992) *Cell* **71,** 671–678
39. Matsubara, M., Yamauchi, E., Hayashi, N. & Taniguchi, H. (1998) *FEBS Lett.* **421,** 203–207
40. Nath, U. & Udgaonkar, J. B. (1997) *Biochemistry* **36,** 8602–8610
41. Linse, S. & Forsén, S. (1995) *Adv. Second Messenger Phosphoprotein Res.* **30,** 89–151
42. Falke, J. J., Drake, S. K., Hazard, A. L. & Peersen, O. B. (1994) *Q. Rev. Biophys.* **27,** 219–290
43. Josefsson, E., McCrea, K., Ní Eidhin, D., O'Connel, D., Cox, J. A., Hook, M., and Foster, T. J. (1998) *Microbiology*, in press

The Binding of Calcium to the B-repeat Segment of SdrD, a Cell Surface Protein of *Staphylococcus aureus*

Elisabet Josefsson, David O'Connell, Timothy J. Foster, Isabelle Durussel and Jos A. Cox

J. Biol. Chem. 1998, 273:31145-31152.
doi: 10.1074/jbc.273.47.31145